APPENDIX Table of Content

Guillon *et al.* Appendix Figure S1

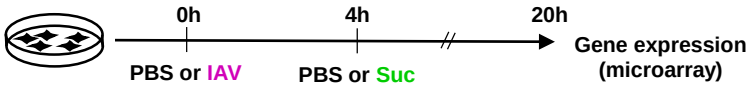

Canonical pathways

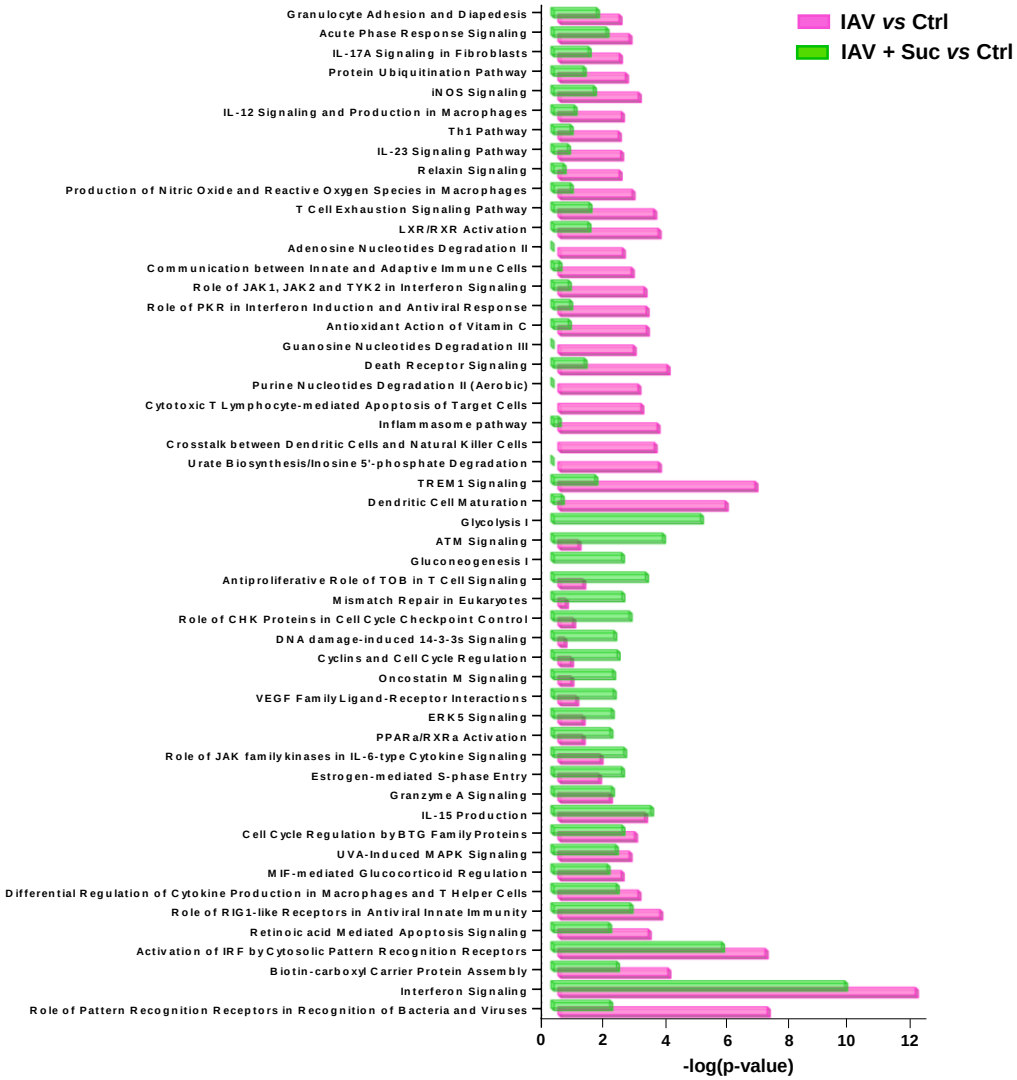

Appendix Figure S1. Effect of succinate on gene expression in influenza virus-infected human bronchial epithelial cells.

Human bronchial epithelial BEAS-2B cells (4 replicates *per* condition) were infected or not ("Ctrl") with the A/Scotland/20/74 (H3N2) virus (IAV) at MOI=1 and were treated or not with succinate (4mg/mL). After 24 h of infection, cells were lysed and total RNA was purified and processed to hybridize pangenomic microarrays. Differentially expressed genes (p-value 2) between two conditions ("IAV-infected cells" *vs*. "control cells" and "IAV-infected cells treated with succinate" *vs*. "control cells") were then selected to perform a gene ontology analysis. Significantly enriched pathways were identified using Ingenuity Pathway Analysis (IPA) and are represented as a bar plot representing the right-tailed Fisher's exact test that was used to calculate a p-value (probability that each canonical pathway assigned to that data set is due to chance alone).

Guillon *et al.* Appendix Figure S2

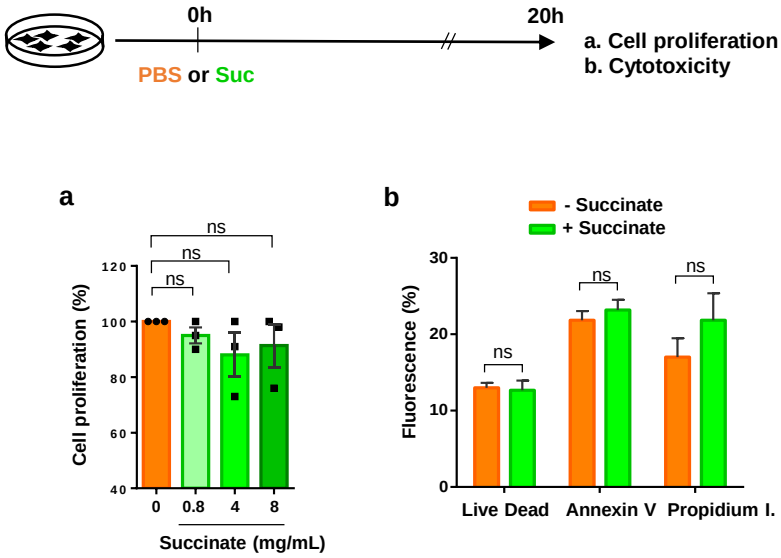

Appendix Figure S2. Succinate is not cytotoxic.

Human bronchial epithelial BEAS-2B cells were treated or not with increasing doses **(a)** or 4 mg/mL **(b)** of succinate for 24 h. Cell proliferation and cytotoxicity were further assessed by an MTS test **(a)** and by flow cytometry using a Live/Dead staining/Annexin V/Propidium Iodide co-staining **(b)**, respectively. Data are represented as the mean ±SEM. Statistical analysis was performed using the Kruskal-Wallis test **(a**, n=3**)** and the multiple t-test **(b**, n=6**)**.

Guillon *et al.* Appendix Figure S3

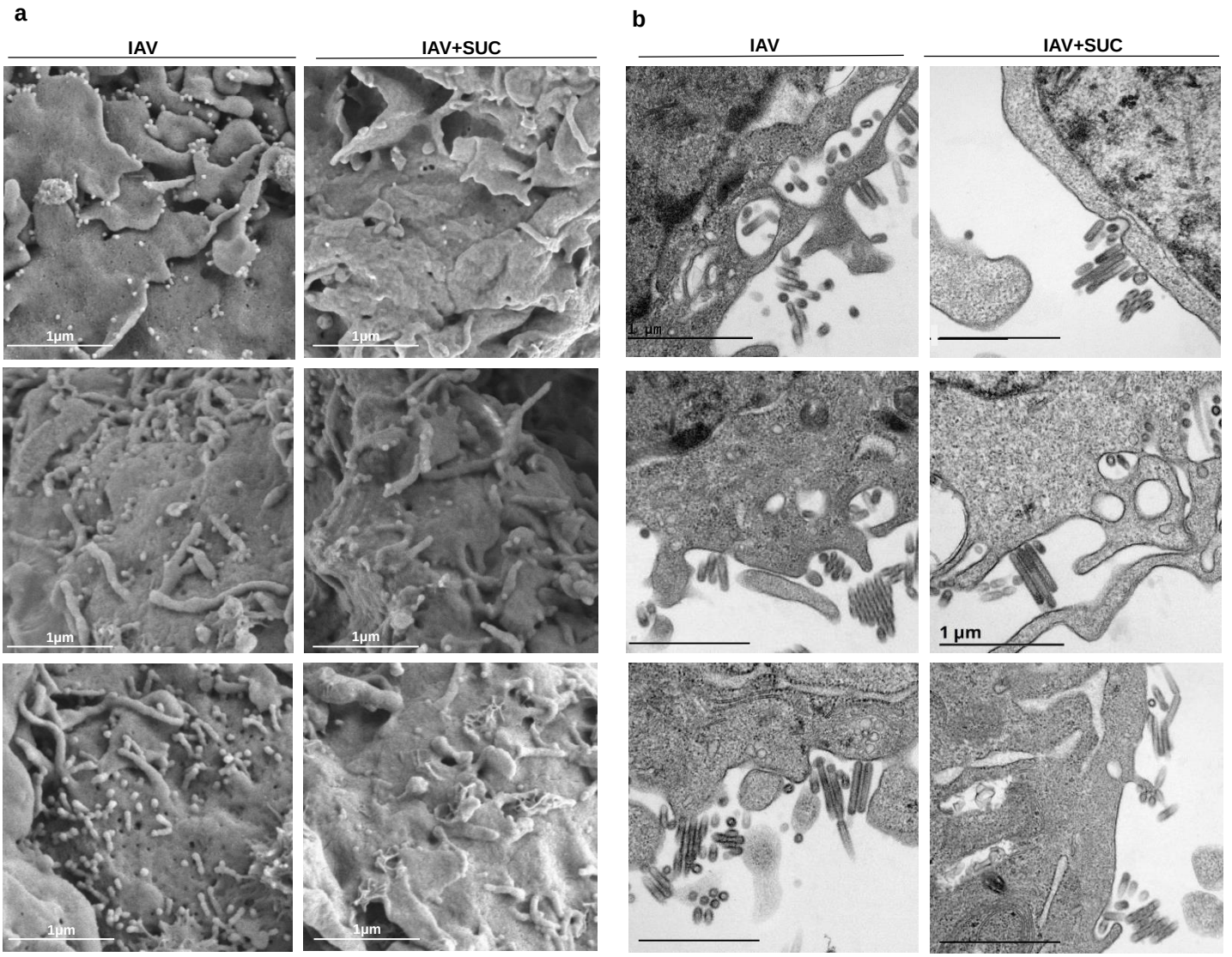

Appendix Figure S3. Scanning and transmission electron microscopy of IAV-infected lung epithelial cells, treated or not by succinate.

Bronchial epithelial (BEAS-2B) cells were infected with influenza A/Scotland/20/74 (H3N2) virus (IAV) at MOI=5 for 4 h and treated or not with succinate (Suc) for 20 h. Scanning **(a)** and transmission **(b)** electron microscopy were used to assess the production of physical viral particles in the supernatants of IAV-infected cells, treated or not with succinate. Scale bar: 1 µM.

Guillon *et al.* Appendix Figure S4

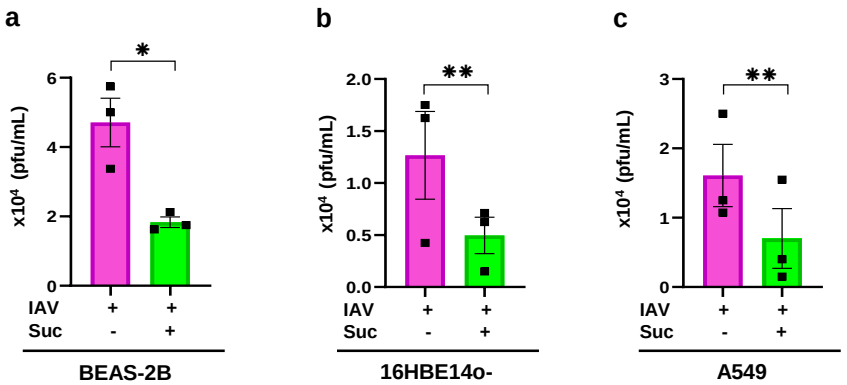

Appendix Figure S4. Antiviral effect of succinate in distinct airway epithelial cell lines.

Human lung epithelial **(a)** BEAS-2B, **(b)** 16HBE14o- or **(c)** A549 cells were infected with influenza A/Scotland/20/74 (H3N2) virus (IAV) at MOI=1 for 4h and treated or not with succinate (Suc) for 20h. Plaque-Forming Units assay determined the production of infectious viral particles in cell supernatants. Data are represented as the mean ± SEM of 3 independent experiments. Statistical analysis was performed using paired t-test.

Guillon *et al.* Appendix Figure S5

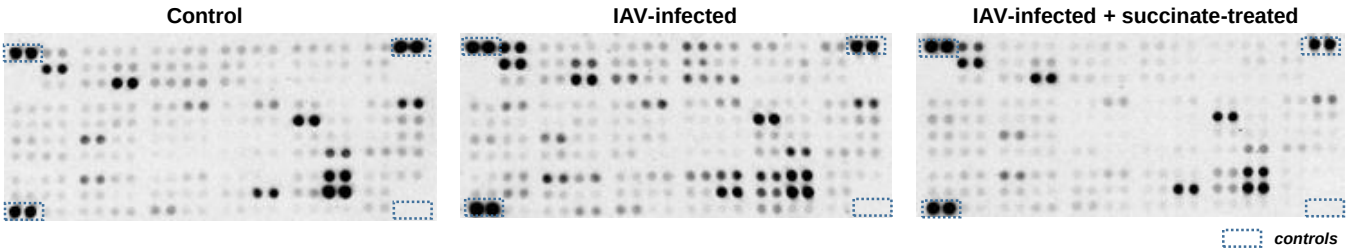

Protein-array coordinates

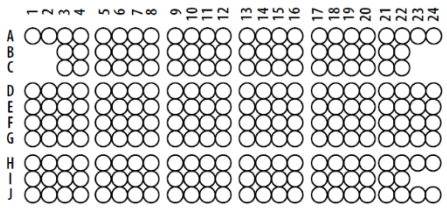

Coordinate	Analyte/Control	Entrez Gene ID	Alternate Nomenclature
A1, A2	Reference Spots	N/A	
A3, A4	Adiponectin/Acrp30	11450	AdipoQ
A5, A6	Amphiregulin	11839	AR, SDGF
A7, A8	Angiopoietin-1	11600	Ang-1, Angpt1
A9, A10	Angiopoietin-2	11601	Ang-2, Angpt2
A11, A12	Angiopoietin-like 3	30924	ANGPT-L3
A13, A14	BAFF/BLyS/TNFSF13B	24099	CD257, TALL1, THANK, ZTNF4
A15, A16	C1q R1/CD93	17064	AA4 Antigen, C1q Rp, CD93
A17, A18	CCL2/JE/MCP-1	20296	MCAF
A19, A20	CCL3/CCL4/MIP-1α/β	20302/20303	
A21, A22	CCL5/RANTES	20304	SISd
A23, A24	Reference Spots	N/A	
B3, B4	CCL6/C10	20305	MRP-1
B5, B6	CCL11/Eotaxin	20292	
B7, B8	CCL12/MCP-5	20293	
B9, B10	CCL17/TARC	20295	
B11, B12	CCL19/MIP-3β	24047	ELC
B13, B14	CCL20/MIP-3α	20297	exodus-1, LARC
B15, B16	CCL21/6Ckine	18829	exodus-2, SCYA21, SLC, TCA-4
B17, B18	CCL22/MDC	20299	ABCD-1, MDC, STCP-1
B19, B20	CD14	12475	
B21, B22	CD40/TNFRSF5	21939	
C3, C4	CD160	54215	Natural killer cell receptor BY55, NK1; NK28
C5, C6	Chemerin	71660	RARRES2, TIG-2
C7, C8	Chitinase 3-like 1	12654	CHI3L1, Cgp39, YKL40
C9, C10	Coagulation Factor III/Tissue Factor	14066	TF, CD142, Thromboplastin
C11, C12	Complement Component C5/C5a	15139	C5/C5a
C13, C14	Complement Factor D	11537	Adipsin, C3 convertase activator, Properdin factor D
C15, C16	C-Reactive Protein/CRP	12944	
C17, C18	CX3CL1/Fractalkine	20312	FKN, Neurotactin
C19, C20	CXCL1/KC	14825	CINC-1; GRO alpha; KC; MGSA-alpha
C21, C22	CXCL2/MIP-2	20310	GROβ, GRO2, CINC-3
D1, D2	CXCL9/MIG	17329	CRG-10, CMK
D3, D4	CXCL10/IP-10	15945	CRG-2, C7
D5, D6	CXCL11/I-TAC	56066	H174, SCYB9B
D7, D8	CXCL13/BLC/BCA-1	55985	
D9, D10	CXCL16	66102	SRPSOX
D11, D12	Cystatin C	13010	ARMD11, CST3, Gamma-trace
D13, D14	DKK-1	13380	Dickkopf-1
D15, D16	DPPIV/CD26	13482	Dpp4, Dipeptidyl-peptidase IV
D17, D18	EGF	13645	Epidermal Growth Factor
D19, D20	Endoglin/CD105	13805	ENG
D21, D22	Endostatin	12822	Col18a1
D23, D24	Fetuin A/AHSG	11625	AHSG, alpha-2-HS-glycoprotein
E1, E2	FGF acidic	14164	FGF-1
E3, E4	FGF-21	56636	
E5, E6	Flt-3 Ligand	14256	Flt3lg
E7, E8	Gas 6	14456	Growth Arrest Specific
E9, E10	G-CSF	12985	Csf3
E11, E12	GDF-15	23886	MIC-1
E13, E14	GM-CSF	12981	Csf2
E15, E16	HGF	15234	Scatter Factor, SF, Hepatopoietin-A
E17, E18	ICAM-1/CD54	15894	
E19, E20	IFN-γ	15978	IFNG
E21, E22	IGFBP-1	16006	
E23, E24	IGFBP-2	16008	

Coordinate	Analyte/Control	Entrez Gene ID	Alternate Nomenclature
F1, F2	IGFBP-3	16009	
F3, F4	IGFBP-5	16011	
F5, F6	IGFBP-6	16012	
F7, F8	IL-1α/IL-1F1	16175	
F9, F10	IL-1β/IL-1F2	16176	
F11, F12	IL-1ra/IL-1F3	16181	IL1RN
F13, F14	IL-2	16183	
F15, F16	IL-3	16187	
F17, F18	IL-4	16189	B cell-stimulatory factor-1
F19, F20	IL-5	16191	
F21, F22	IL-6	16193	
F23, F24	IL-7	16196	
G1, G2	IL-10	16153	CSIF
G3, G4	IL-11	16156	
G5, G6	IL-12 p40	16160	
G7, G8	IL-13	16163	
G9, G10	IL-15	16168	
G11, G12	IL-17A	16171	
G13, G14	IL-22	50929	IL-TIF
G15, G16	IL-23	83430	
G17, G18	IL-27 p28	246779	
G19, G20	IL-28A/B	330496/338374	
G21, G22	IL-33	77125	NF HEV, DVS 27
G23, G24	LDL R	16835	low density lipoprotein receptor
H1, H2	Leptin	16846	OB
H3, H4	LIF	16878	
H5, H6	Lipocalin-2/NGAL	16819	Siderocalin, 24p3
H7, H8	LIX	20311	CXCL5, GCP-2, ENA-78
H9, H10	M-CSF	12977	CSF-1
H11, H12	MMP-2	17390	Gelatinase A
H13, H14	MMP-3	17392	Stromelysin-1
H15, H16	MMP-9	17395	Clg4b, Gelatinase B, GELB
H17, H18	Myeloperoxidase	17523	MPO
H19, H20	Osteopontin (OPN)	20750	Eta-1, Spp1
H21, H22	Osteoprotegerin/TNFRSF11B	18383	OPG, Ocif
H23, H24	PD-ECGF/Thymidine phosphorylase	72962	dThdPase, ECGF1, Gliostatin, MEDPS1, MNGIE
I1, I2	PDGF-BB	18591	
I3, I4	Pentraxin 2/SAP	20219	PTX2
I5, I6	Pentraxin 3/TSG-14	19288	PTX3
I7, I8	Periostin/OSF-2	50706	Fasciclin I-like, POSTN, TRIF52
I9, I10	Pref-1/DLK-1/FA1	13386	DLK1, pG2, ZOG
I11, I12	Proliferin	18811	MRP
I13, I14	Proprotein Convertase 9/PCSK9	100102	NARC-1
I15, I16	RAGE	11596	AGER
I17, I18	RBP4	19662	Retinol-Binding Protein 4
I19, I20	Reg3G	19695	PAP3
I21, I22	Resistin	57264	ADSF, FIZZ3
J1, J2	Reference Spots	N/A	
J3, J4	E-Selectin/CD62E	20339	ELAM1, LECAM2, Sele
J5, J6	P-Selectin/CD62P	20344	GMP-140, LECAM3, Selep
J7, J8	Serpin E1/PAI-1	18787	Nexin, PLANH1
J9, J10	Serpin F1/PEDF	20317	EPC-1
J11, J12	Thrombopoietin	21832	Tpo, MGDF
J13, J14	TIM-1/KIM-1/HAVCR	171283	
J15, J16	TNF-α	21926	TNFSF1A
J17, J18	VCAM-1/CD106	22329	
J19, J20	VEGF	22339	VEGF-A, VPF
J21, J22	WISP-1/CCN4	22402	
J23, J24	Negative Control	N/A	

Appendix Figure S5. Datasheet of mouse XL cytokine array kit.

Upper panels: High resolution scans of original mouse XL cytokine arrays, *Middle panel*: overlay template and coordinates; *Lower panels*: reading appendix.

Guillon *et al.* Appendix Figure S6

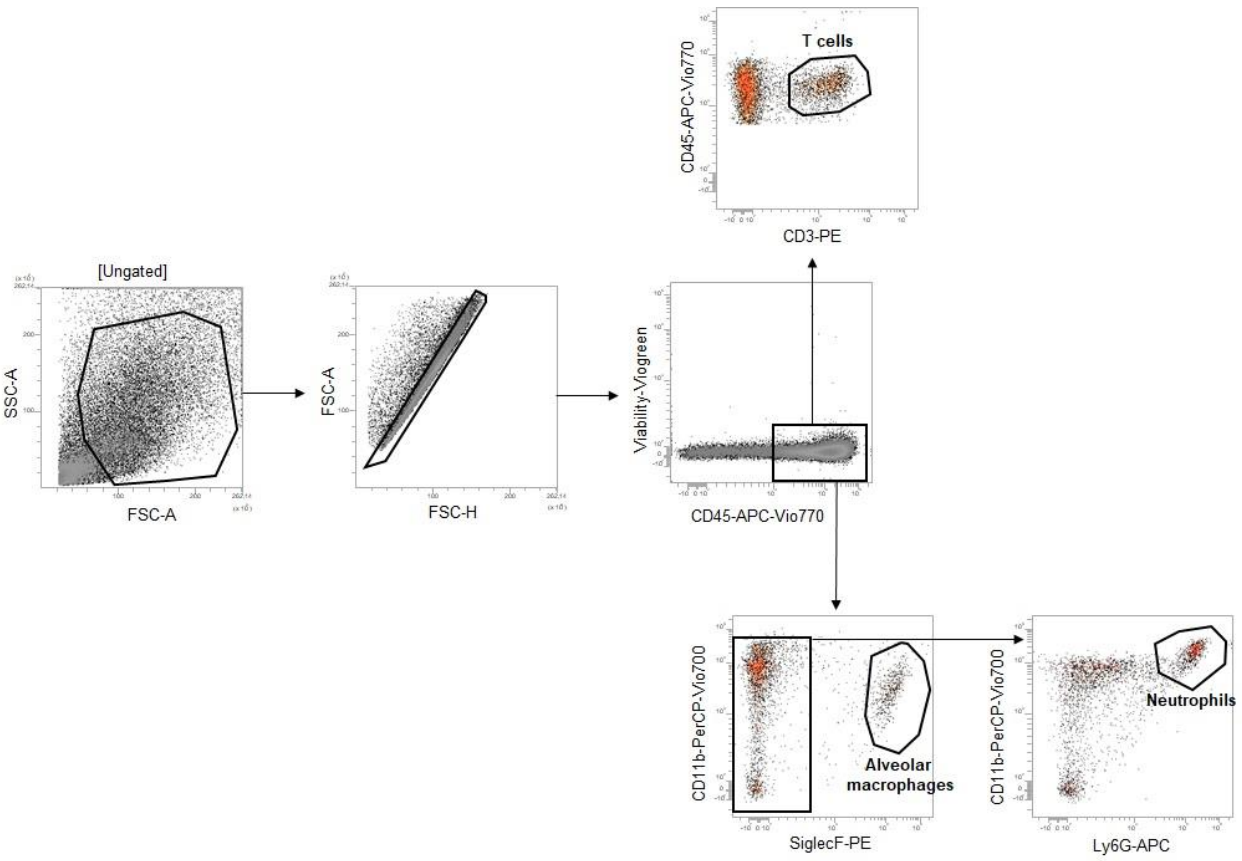

Appendix Figure S6. Flow cytometry gating strategy.

Surface gating used to define immune cell subsets in Figure 4.

Guillon *et al.* Appendix Figure S7

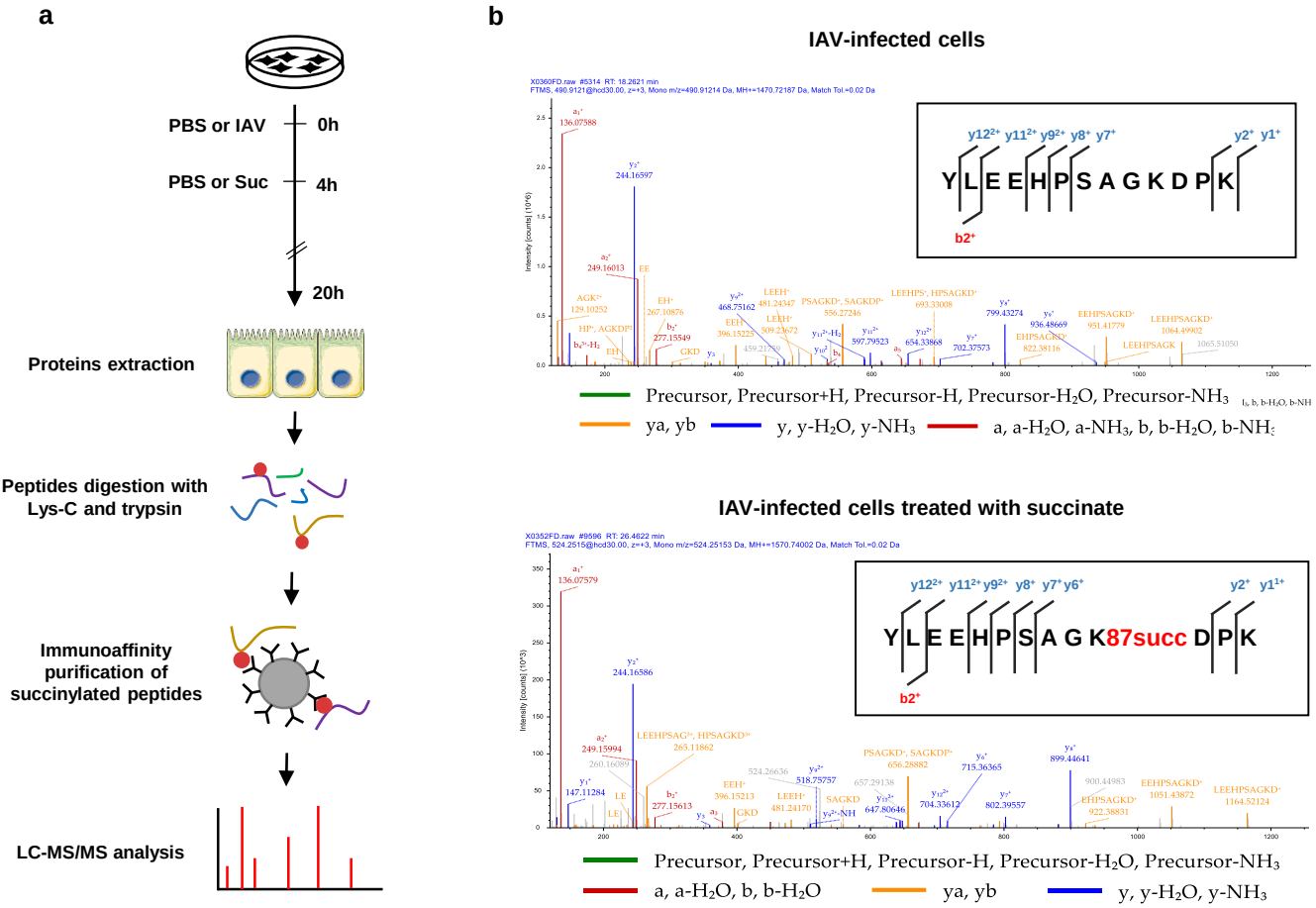

Appendix Figure S7. Mass spectrometry methodology and profiles.

(a) Human bronchial epithelial BEAS-2B cells were infected with A/Scotland/20/74 (H3N2) virus (IAV) at MOI=1 for 4 h, and subsequently treated or not with 4 mg/mL of succinate for 20 h. Cells were lysed and proteins were digested to peptides with Lys-C and trypsin. Succinylated peptides were isolated directly from protease-digested cellular protein extracts by immunoaffinity purification (IAP) using an antibody specific for the succinyl-Lysine motif, and the modified peptides were further analyzed by LC-MS/MS. **(b)** Representative MS/MS spectra of succinylated and non-succinylated NP peptides.

Guillon *et al.* Appendix Figure S8

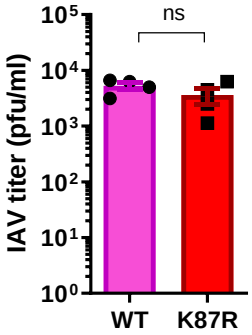

Appendix Figure S8. Similar growth of wild-type K87 and mutant K87R IAV strains.

Human bronchial epithelial BEAS-2B cells were infected with influenza A/Scotland/20/74 (H3N2) (IAV) strains carrying a wild-type NP ("WT") or a NP with a K87R substitution ("K87R"). Cells were infected by either virus at MOI=1 for 4 h, then washed and left untreated for 20 h. Plaque-Forming Units assay determined the production of infectious viral particles in cell supernatants. Data are represented as the mean ± SEM of 4 independent experiments. Statistical analysis was performed using the Mann-Whitney test.

Guillon *et al.* Appendix Figure S9

	1- NP K87	2- NP K87E	3- NP K87 succinylated
NP structure	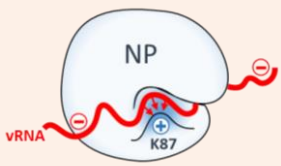	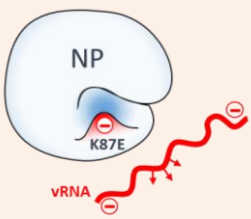	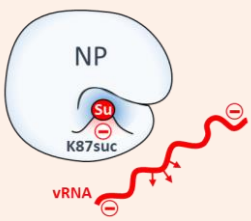
Charge of the K87 residue	**+**	**-**	**-**
NP-vRNA interaction	**+++**	**+**	**+**

Appendix Figure S9. Impact of the NP structure on its interaction capacity with viral RNA.

Panel 1: In NP, the Lysine (K)87 is a positively charged amino acid which is key in the interaction with negatively charged vRNA. *Panel 2:* Conversely, glutamic acid (E) is a negatively charged residue. As a result, NP K87E mutant interacts less with vRNAs. *Panel 3:* In succinate-treated cells, the addition of a succinyl group to the NP K87 residue neutralizes the positive charge of lysine and imparts a negative charge, thus altering the NP-vRNA interaction as well.

Guillon *et al.* Appendix Table S1

REAGENT OR RESOURCE	SOURCE	IDENTIFIER
Antibodies		
Anti-Influenza A Virus Nucleoprotein antibody	Abcam	ab128193
Anti-Influenza A Virus Nucleoprotein antibody FITC	Abcam	ab20921
Anti-NP mAb clone 3/1	Gift from Dr Webby, St Jude Hospital, Memphis, USA	N/A
Anti-Influenza A M1 antibody	Abcam	ab22396
Anti-Influenza A NEP/NS2 antibody	Invitrogen	PA532235
Anti-Influenza A PA antibody	Invitrogen	PA532223
Anti-Influenza A M2 antibody	Santa Cruz Biotechnology	sc-32238
Anti-Influenza A PB2 antibody	Invitrogen	PA532220
Anti-Influenza NS1 antibody	Gift from Dr Marc, INRAE, Nouzilly, France	N/A
Anti-CRM1 antibody	BD Biosciences	611832
beta Actin Monoclonal Antibody	ThermoFisher Scientific	MA5-15739
Anti-Mouse IgG (whole molecule)–Peroxidase antibody	Sigma-Aldrich	A9044
Anti-Rabbit IgG (whole molecule)–Peroxidase antibody	Sigma-Aldrich	A9169
Anti-Mouse IgG1 Secondary Antibody, Alexa Fluor 488	ThermoFisher Scientific	A21121
Anti-Rabbit IgG Secondary Antibody, Alexa Fluor 488	ThermoFisher Scientific	A11008
APC-eFluor780-conjugated anti-CD45 (30-F11)	ThermoFisher Scientific	47-0451-82
FITC-conjugated anti-Ly6G (1A8)	BioLegend	127605
PerCP-Cy5.5-conjugated anti-CD11b (M1/70)	BioLegend	101227
APC-conjugated anti-CD11c (N418)	BioLegend	117309
PECy7-conjugated anti-CD3e (145-2C11)	BD Pharmingen	552774
PE-conjugated anti-Siglec F (E50–2440)	BD Pharmingen	552126
Vioblue-conjugated anti-F4/80 (clone BM8)	ThermoFisher Scientific	48-4801-82
Chemicals, peptides		
Poly(I:C) LMW 25mg	Invivogen	tlrl-picw
Disodium succinate	Sigma-Aldrich	W327700
Sodium malonate dibasic monohydrate	Sigma-Aldrich	M4795
Leptomycin B	Enzo Life Sciences	ALX-380-100-C100
Lipofectamine™ LTX Reagent with PLUS™ reagent	Invitrogen	15338030
ActinRed™ 555 ReadyProbes™ Reagent	ThermoFisher Scientific	R37112
NucBlue™ Fixed Cell ReadyProbes™ Reagent	ThermoFisher Scientific	R37606
2'-(4-Methylumbelliferyl)-α-D-N-acetylneuraminic acid sodium salt hydrate	Chemodex	M0096
Protease Inhibitor Cocktail	Sigma Aldrich	P8340
GibcoTM Ham's F-12 Nutrient Mix	Fisher Scientific	31765027
GibcoTM MEM	Fisher Scientific	31095029
GibcoTM DMEM	Fisher Scientific	11594446
Trypsin 0.25 %/EDTA 0.02 % in PBS	PAN BIOTECH	P10-020100
Trypsin, TPCK Treated	ThermoFisher Scientific	20233
Trypsin / Lys-C Mix, Mass Spec Grade	Promega	V5072
MEM Eagle with Earle's BSS (2X)	Lonza	BE12-668F
Crystal Violet Oxalate	RAL Diagnostics	361490
Formaldehyde, 37 wt % sol. in water, stab. with 5-15% methanol	Acros Organics	119690010
Avicel® RC 581 Stabilizer	FMC BioPolymer	N/A
Annexin V-FITC kit	Miltenyi Biotech	130-092-052
Propidium Iodide Solution	Miltenyi Biotech	130-093-233
True-Nuclear™ Transcription Factor Buffer Set	Biolegend	424401
BD Cytofix/Cytoperm™ Fixation/Permeabilization Solution Kit	Fisher Scientific	BDB554714
Red Blood Cell Lysing Buffer Hybri-Max™	Sigma Aldrich	R7757
TB Green® Premix Ex Taq™	Takara	RR420L
50% EM Glutaraldehyde	TAAB Laboratory Equipment	G045
Uranyl acetate	Merck	8473
Osmium tetroxide 4% solution	Electron Microscopy Science	19150
Propylene oxide	Alfa Aesar	30765
Epon™ MNA substitute	Sigma Aldrich	45347
Commercial Assays		
LIVE/DEAD™ Fixable Aqua Dead Cell Stain Kit	ThermoFisher Scientific	L34966
CellTiter 96® AQueous One Solution Cell Proliferation Assay	Promega	G3582
Pierce™ BCA Protein Assay Kit	ThermoFisher Scientific	23225
Phusion™ High-fidelity DNA polymerase	Fisher Scientific	16237911
Nucleospin® RNA	Macherey-Nagel	740955
High Capacity cDNA reverse transcription kit	Applied Biosystems	4368813
Human IL6 ELISA DuoSet	R&D Systems	DY206
Human IL8 ELISA DuoSet	R&D Systems	DY208
Human IP-10 ELISA DuoSet	R&D Systems	DY266
Human RANTES ELISA DuoSet	R&D Systems	DY278
Mouse IL6 ELISA DuoSet	R&D Systems	DY406
Mouse KC ELISA DuoSet	R&D Systems	DY453
Mouse MPO ELISA DuoSet	R&D Systems	DY3667
Human Cytokine Array Kit	R&D Systems	ARY005B
Mouse XL Cytokine Array	R&D Systems	ARY028
PTMScan® Succinyl-lysine Motif	Cell Signaling	13764
SurePrint G3 human gene expression microarray kit	Agilent Technologies	G4851C
Low Input Quick Amp labeling kit	Agilent Technologies	5190-2308
Consumables		
3 mm High Throughput NMR Tube	CortecNet	WG-3000-7-50
C18 Nano Trap Columns	Thermo Scientific	164535
C18 Acclaim PepMap RSLC Columns	Thermo Scientific	164540
Sep-Pak tC18 6 cc Vac Cartridge	Waters	186004621
Gentle MACSTM M tube	Miltenyi Biotech	130-093-236
Experimental Models		
C57BL/6	Janvier	C57BL/6JRjFEMELLESPF4
BEAS-2B	ATCC®	CRL-9609
A549	ATCC®	CCL-185
MDCK.2	ATCC®	CRL-2935
HEK293T	ATCC®	CRL-11268
16HBE14o-	Sigma-Aldrich	SCC150
Influenza A/Scotland/20/74	Pasteur Institute, France	N/A
Influenza A/WSN/33 wild type and NS1flag-tagged	INRAE, Jouy-en-Josas, France	N/A
Influenza A/PR8 wild type and delta NS1	FFreiburg University, Germany	N/A
Softwares		
GraphPad Prism	GraphPad Software	https://www.graphpad.com/scientific-software/prism/
VenturiOne	Applied Cytometry	https://www.appliedcytometry.com/venturi/
FUJI FILM Multigauge	Bioz	https://www.bioz.com/
LightCycler 480 SW V.1.5	Roche	https://lifescience.roche.com/
ImageJ	Imagej	https://imagej.net/Welcome
BioStation IM software (v2.12)	Nikon	https://www.nikon.com/products/microscope-solutions/
Leica LasX Life Sciences	Leica Microsystems	https://www.leica-microsystems.com
Digital Micrograph V.3	Gatan	https://www.gatan.com/products/tem-analysis
AMIX software package (Analysis of MIXture, version 3.9.14)	Bruker Biospin	https://www.bruker.com/products/mr/nmr/software/amix
SIMCA 13.0.3 software	Umetrics	https://umetrics.com/kb/simca-1303
ChenomX NMR Suite 8.1	ChenomX	https://www.chenomx.com/products/
MetaboAnalyst	MetaboAnalyst	https://www.metaboanalyst.ca/
Topspin version 3.6 software	Bruker Daltonik	https://www.bruker.com/products/mr/nmr/software/topspin
GeneSpring software	Agilent Technologies	https://www.agilent.com/
Ingenuity Pathways Analysis (IPA) software	Qiagen	https://digitalinsights.qiagen.com/
Feature Extraction software version 10.7.3.1	Agilent Technologies	https://www.agilent.com/
Post Run Analysis software	Shimadzu	https://www.shimadzu.com
myProMS (Vesrion 3.9)	LSMP, Institut Curie, France	https://pubmed.ncbi.nlm.nih.gov/17610305/
Xcalibur software	Thermo Scientific	https://www.thermofisher.com
Seahorse Wave Controller Software	Agilent	https://www.agilent.com
Seahorse Wave Desktop Software	Agilent	https://www.agilent.com
R software (Version 3.4.4)	r-project	https://www.r-project.org/
Omnilog Data Collection 2.4	Biolog	https://www.biolog.com
PM-M Kinetic and PM-M Parametric	Biolog	https://www.biolog.com